Discover Concrete and Cement

RESEARCH Open Access

Influence of chemical activation on the strength and durability of lime–corn cob ash cement

Odiwuor Vincent Onyango[1*], Stephen S. Barasa[1] and Zipporah Onyambu[1]

*Correspondence:
Odiwuor Vincent Onyango
vincentodiwuor623@gmail.com
[1]Department of Chemistry and Biochemistry, University of Eldoret, P.O. Box 1125-301, Eldoret, Kenya

Abstract

The slow rate of strength gain and the relatively poor durability of lime–pozzolana binders limit their broader use in sustainable construction applications. This study examined how chemical activation influences the physicochemical characteristics, compressive strength, porosity, and sulfuric acid resistance of lime–corn cob ash (CCA) mortars. CCA was analyzed using X-ray fluorescence (XRF), X-ray diffraction (XRD), Fourier transform infrared spectroscopy (FTIR), and electrical conductivity tests to evaluate its pozzolanic behavior. Mortars containing a 50:50 lime–CCA ratio were prepared using water, 0.5 M NaOH, and 0.5 M Na_2SO_4 as mixing media. The results indicated that CCA is rich in silica (61.61% SiO_2), with a combined SiO_2 + Al_2O_3 + Fe_2O_3 content of 72.19%, confirming its suitability as a pozzolanic material. The reduction in electrical conductivity of about 28.1% after 240 min suggests moderate pozzolanic reactivity of CCA. Chemical activation markedly enhanced performance. Compressive strength increased from 2.91 MPa in the non-activated system to 5.92 MPa and 7.77 MPa for Na_2SO_4 and NaOH-activated mortars, respectively. Porosity showed a decreasing trend from L100–H_2O to LCCA50–0.5 M NaOH. Under sulfuric acid exposure, activated mortars experienced lower mass and strength losses than non-activated ones, with NaOH activation providing the best resistance. In contrast, pure lime mortar fully disintegrated under acidic conditions. The results confirm that chemical activation significantly improves the mechanical performance and durability of lime–CCA binders. The study demonstrates the viability of corn cob ash as a sustainable pozzolanic material for low-carbon, non-structural construction applications and highlights the effectiveness of different chemical activators in enhancing lime-based systems.

Keywords Corn cob ash, Lime-pozzolana binder, Chemical activation, Pozzolanic reactivity, Sulfuric acid resistance, Sustainable construction materials, Agricultural waste valorization

1 Introduction

Cement production is essential for modern infrastructure development and underpins the global construction industry. However, the construction industry is increasingly challenged by the environmental impacts of conventional cement production, particularly its high carbon emissions and energy consumption [1]. Ordinary Portland cement

(OPC) manufacturing is a major contributor to global CO_2 emissions, releasing approximately 0.8 tons of CO_2 per ton of cement produced, primarily due to limestone calcination and fossil fuel combustion. The process is also highly energy-intensive, requiring approximately 2.5–4.0 GJ per ton of cement. Extraction of raw material used in OPC production contributes to environmental degradation, including land depletion and biodiversity loss [2–4]. These concerns have intensified the need for sustainable and low-carbon alternatives in the construction sector [5].

Lime-based binders have gained attention as low-carbon materials, particularly for their compatibility with pozzolanic additives and suitability in specific construction applications [6]. Lime–pozzolan cements were historically the main binders used in iconic architectural structures and continue to play a vital role in the conservation of heritage masonry [7]. Their inherent chemical compatibility and permeability allow restoration works to preserve the original material of historic buildings rather than merely repairing visible damage. Even today, this material is employed in the restoration of both historic and contemporary monuments in accordance with established conservation principles [8, 9]. However, their practical application remains limited by inherent drawbacks, including prolonged setting time, slow strength development, and poor durability in aggressive environmental conditions, which may compromise the effectiveness of restoration work. [7, 8]. These limitations are primarily attributed to the low reactivity of lime–pozzolan systems, which restricts their use in structural applications despite their environmental benefits [9].

To address some of these challenges, significant research has focused on the incorporation of pozzolans, including industrial by-products such as fly ash, silica fume, volcanic ash, ground granulated blast furnace slag, and red mud, into lime mortars [4, 9]. These industrial byproducts have been shown to enhance durability and mechanical strength, while also offering the added benefit of improved environmental sustainability [10]. Incorporating SCMs into cement systems helps address two key challenges at once. It reduces greenhouse gas emissions and diverts industrial waste from landfills, supporting circular economy principles and contributing to global sustainability goals such as SDG 7, SDG 9, and SDG 12 [4]. However, these materials often face issues relating to unpredictability in composition, long-term performance uncertainty, and regulatory limits [11]. In addition, getting natural pozzolans with homogeneous quality is typically challenging, which inhibits their broader application [12].

In response, agricultural residues have gained attention as alternative pozzolanic materials due to their abundance and potential for sustainable utilization. The use of agricultural by-products addresses waste disposal challenges while providing a sustainable alternative to conventional materials in the cement industry [13]. Agro-based wastes, including rice husk ash (RHA), sugarcane bagasse ash, and corncob ash (CCA), have attracted considerable interest due to their ability to improve concrete performance while lowering environmental impact [14–20]. Recent research has broadened the range of agricultural residues investigated for cementitious applications to include de-oiled sesame and sunflower seed residues [21] and ashes derived from cotton and flaxseed oilseed extracts [22]. These studies reflect the growing interest in valorizing agricultural wastes as sustainable cementitious materials. Beyond agricultural residues, metakaolin (MK) has recently gained attention as a reactive pozzolanic material. Khan et al. [23]. reported that partial MK replacement enhanced the mechanical and durability

performance of concrete, with 15% replacement providing favorable strength, permeability, water absorption, and chloride resistance. Similarly, Khan et al. [24]. demonstrated that alkali-activated masonry containing MK and GGBS achieved high compressive strength, low water absorption, and good acid resistance. These findings highlight the potential of calcined clays and industrial by-products for developing durable and lower-carbon cementitious materials [25].

Corn cob ash has shown considerable promise owing to its high silica content and pozzolanic characteristics. Corncobs are generated in large quantities as by-products of global maize production, yet they are often disposed of through open burning or left to decompose, contributing to environmental pollution [26, 27]. Converting corncobs into ash for use in cementitious systems offers a sustainable pathway for waste valorization while reducing reliance on conventional cement. This approach significantly reduces the carbon footprint of conventional cement production, which is critical considering the sector's major contribution to global carbon dioxide emissions [28]. Chemically, CCA typically contains high proportions of silica and alumina, which are essential for pozzolanic reactions, enabling the formation of cementitious compounds that enhance strength and durability [29, 30].

Despite these advantages, the performance of lime–CCA binders remains constrained by slow pozzolanic reaction kinetics and incomplete utilization of the reactive amorphous phases present in corn cob ash, resulting in delayed formation of strength-giving hydration products [31]. Chemical activation has emerged as a promising approach for overcoming these limitations by enhancing the dissolution of reactive silica and alumina, thereby accelerating the formation of calcium silicate hydrate (C–S–H) and calcium aluminate hydrate (C–A–H) phases that improve both mechanical performance and matrix densification [32–35]. Although previous studies have reported improved strength following chemical activation, most have investigated individual activators under different mix proportions, activator dosages, curing regimes, and testing conditions, making direct comparison of activator performance difficult [36, 37]. Furthermore, existing research has focused predominantly on strength development, with comparatively little attention given to durability under aggressive exposure conditions.

Chemical activation using sodium hydroxide (NaOH) and sodium sulfate (Na_2SO_4) has been widely investigated in alkali-activated and blended cement systems containing industrial by-products such as slag [38], fly ash [39], and volcanic ash [40]. However, these findings cannot be directly extrapolated to lime-agricultural ash binders because their hydration mechanisms, calcium availability, and reaction pathways differ substantially. Research on CCA has likewise concentrated mainly on geopolymer binders activated with sodium silicate under elevated-temperature curing [41], whereas ambient-cured lime–CCA systems remain largely unexplored. Consequently, there is limited understanding of how different chemical activators influence both the mechanical and durability performance of lime–CCA binders under identical experimental conditions.

To address this knowledge gap, the present study provides a controlled comparative evaluation of NaOH and Na_2SO_4 as chemical activators for ambient-cured lime–CCA binders using the same binder composition, activator concentration, curing conditions, and testing procedures. Unlike previous studies that evaluated activators independently, this work isolates the effect of activator type, enabling a direct assessment of their relative effectiveness. Beyond compressive strength, the study integrates physicochemical

characterization of CCA with porosity measurements and sulfuric acid resistance to establish the relationships between chemical activation, mechanical performance, and durability. This integrated approach advances current knowledge by demonstrating not only whether chemical activation improves lime–CCA binders but also how different activation mechanisms influence long-term performance under aggressive conditions. The findings therefore provide new scientific insight into the selection of chemical activators for sustainable lime–pozzolan systems and contribute practical guidance for the development of durable, low-carbon construction materials derived from agricultural waste.

Accordingly, the objective of this study is to directly compare the effects of NaOH and Na_2SO_4 on the mechanical and durability performance of lime–CCA binders under identical conditions. It is hypothesized that both activators will enhance the pozzolanic reactivity of CCA relative to the nonactivated binder but that their distinct activation mechanisms will produce different levels of strength development, porosity refinement, and resistance to sulfuric acid attack. By presenting controlled side-by-side evaluation of these two widely used activators within the same lime–CCA system while simultaneously assessing strength, porosity, and acid durability, this work provides a more comprehensive understanding of chemical activator performance and supports the development of durable, low-carbon lime–pozzolan binders derived from agricultural waste. The study contributes to a clearer understanding of the effectiveness of different chemical activators in improving the performance of lime-based binders while supporting sustainable material development.

2 Materials and methods

2.1 Materials

The primary materials utilized in this research included hydrated lime (HL), CCA, and standard sand. The raw maize cobs were obtained from local farmers in Uasin Gishu County, Kenya, a prominent maize-producing region. To maintain experimental consistency and minimize variations in chemical properties, all cobs were sourced from the same maize variety and harvested during the same agricultural season. Commercial-grade hydrated lime ($Ca(OH)_2$) served as the primary binder for the mortar mixtures. Standard sand was used as the fine aggregate, with a maximum particle size of 5 mm, a specific gravity of 2.62, and a fineness modulus of 3.12. The particle size distribution of the sand is illustrated in Fig. 1. For the chemically activated series, analytical-grade sodium hydroxide (NaOH) and sodium sulfate (Na_2SO_4) pellets were used to prepare the 0.5 M activating solutions. All mixtures and chemical solutions were prepared using potable water. Hydrated lime was supplied as a powder with a purity of 98%, while NaOH and Na_2SO_4 were obtained in pellet and powder forms with purities of 97% and 99%, respectively.

2.2 Methods

2.2.1 Preparation and calcination of corn cobs

The raw corn cobs were thoroughly washed with tap water to eliminate soil, organic debris, and residual pesticides that could introduce deleterious impurities into the resulting ash. Following cleaning, the cobs were oven-dried at 105 °C for 24 h to remove all moisture. To enhance thermal efficiency during combustion, the dried cobs were

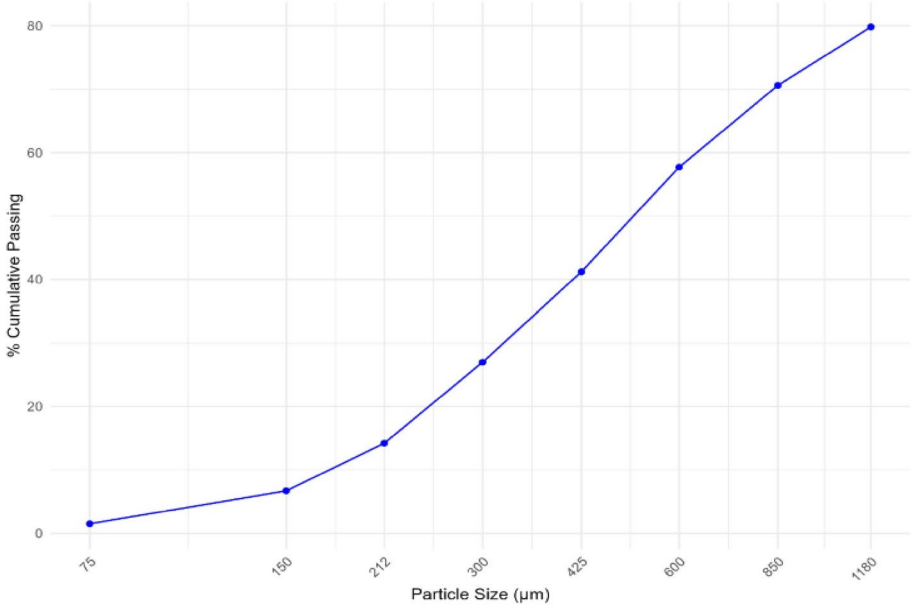

Fig. 1 Grain size distribution curve of the river sand

mechanically shredded with a mill for grinding animal feed into granules smaller than 6 mm in diameter. The fragments were then subjected to a controlled calcination process in a muffle furnace, where they were heated at a constant temperature of 700 °C for a duration of 3 h. This temperature was specifically selected to ensure the production of ash with a high amorphous silica content. After calcination, the CCA was allowed to cool to room temperature within the furnace to avoid thermal shock. To achieve the required fineness and optimize pozzolanic reactivity, the ashes underwent a mechanical grinding process using a laboratory-scale ball mill. The materials were milled for a duration of 60 min at 200 rpm to ensure a uniform particle-size distribution. This grinding duration was selected to achieve a fine powder capable of passing through a 75 µm sieve to maximize the specific surface area available for pozzolanic activity. The ash yield obtained represented 11.70% of the original mass of the corn cob. The final CCA was stored in airtight containers to prevent moisture absorption and pre-hydration prior to its incorporation into the mortar mixtures.

2.2.2 Physical and chemical properties characterization

The chemical composition of the CCA was determined using X-ray fluorescence (XRF) analysis using a Bruker XRF-S8 Tiger spectrometer. For Loss on Ignition (LOI) determination, CCA samples were first oven-dried at 105 °C for 24 h to achieve a constant mass. 1 g of the dried sample was then heated in a muffle furnace at 900 °C for 60 min to ensure complete combustion of residual carbon. After cooling in a desiccator to prevent moisture uptake, the final mass was recorded. The LoI was calculated as the percentage mass loss relative to the initial dry weight. All tests were conducted in replicates to ensure reliability and accuracy of the results. The composition of CCA and HL used in this study is given in Table 2. Fourier-transform infrared (FTIR) spectroscopy, using a Perkin-Elmer instrument with a resolution of 3 cm^{-1}, was employed to identify the vibrational stretching and bending characteristics of silica within the samples. The crystalline phases of the corn cob ash were characterized by X-ray diffraction (XRD) using a Bruker D8 Advance

diffractometer over a 2θ range of 10 ° to 90 °, with a step size of 0.02 °, utilizing Cu Kα radiation (λ = 1.5406 Å). The resulting diffraction pattern is presented in Fig. 2.

2.2.3 Pozzolanic activity test

The pozzolanic activity test was conducted following the method described by Musyimi et al. [42]. Initially, 200 cm^3 of distilled water was placed in a glass beaker and heated to 40 ± 1 °C using a hot plate equipped with a magnetic stirrer. Subsequently, 0.8 g of calcium hydroxide was added to the water to prepare a saturated solution, which was stirred for two minutes to ensure proper mixing. The electrical conductivity of this saturated calcium hydroxide solution was then measured using a conductivity meter. Thereafter, 5.0 g of a finely ground pozzolana sample was introduced into the solution, which was maintained at 40 ± 1 °C. The mixture was continuously stirred for an additional 2 min. Electrical conductivity measurements were recorded at 30-min intervals over a period of 4 h. Pozzolanic activity was evaluated based on the difference between the conductivity of the saturated calcium hydroxide solution and that of the pozzolana-containing solution. All experiments were performed in triplicate, and the average values were reported.

2.2.4 Binder formulations

The mortar mixtures were formulated using HL as the primary binder, with CCA incorporated as a supplementary pozzolanic material. The blended binder was prepared by replacing 50% of the hydrated lime with corn cob ash (CCA) on a mass basis, resulting in a 1:1 lime-to-CCA ratio (LCCA50). This replacement level was selected based on previous lime–pozzolan studies by Játiva et al. [43]. and Sales et al. [44], which demonstrated the effective performance of lime–pozzolana binders at a 1:1 lime-to-pozzolana ratio. This ratio provides a suitable balance between the calcium hydroxide supplied by lime and the reactive silica and alumina contributed by the pozzolan, thereby promoting the formation of cementitious products while maintaining satisfactory workability and mechanical performance. A control mixture consisting of 100% HL was also prepared for comparative analysis. All mortar specimens were designed with a constant binder-to-fine aggregate ratio of 1:3 (450 g of binder to 1350 g of standard sand) and a

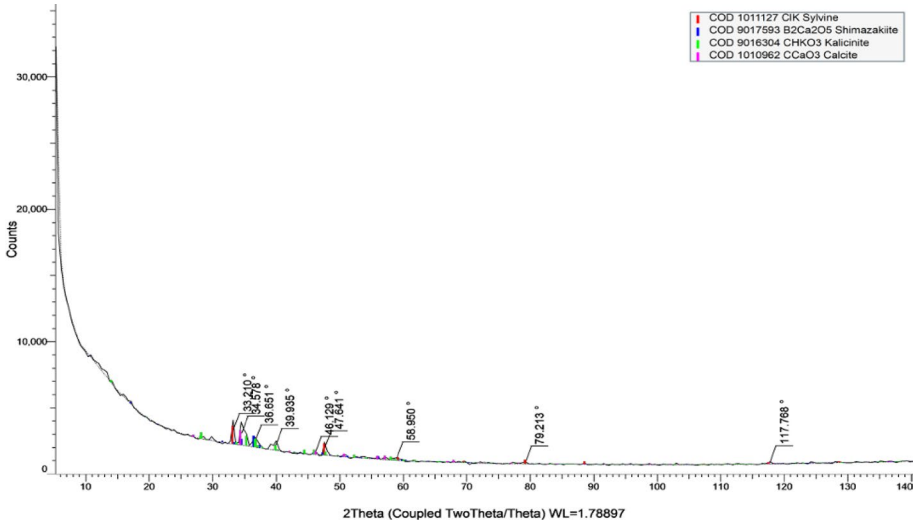

Fig. 2 XRD pattern of CCA

liquid-to-binder (L/B) ratio of 0.55. The detailed mix proportions, including the specific chemical activators used for each series, are summarized in Table 1.

2.2.5 Mixing casting and curing

Mortar preparation and curing were conducted in accordance with KS EAS 148–1:2000 [45], with specific modifications to accommodate the lime–pozzolana system. The binder consisted of an HL and CCA mixture in a 1:1 weight ratio (designated as LCCA50), while a pure hydrated lime mix (L100) served as the control. Depending on the mix design, the mixing liquid consisted of either potable water, 0.5 M NaOH, or 0.5 M Na_2SO_4. A concentration of 0.5 M was selected based on previous studies by Marangu et al. [36]. and Mwiti et al. [32]., reporting its effectiveness in enhancing the pozzolanic reaction of lime–pozzolan systems while maintaining stable mortar properties. A single concentration was intentionally used for both activators to enable a direct comparison of their relative effectiveness under identical experimental conditions. The objective of this study was to evaluate the influence of the type of chemical activator rather than to optimize activator concentration. Mixing was performed using a trowel. The dry binder and sand were initially homogenized for 1 min, after which the designated liquid was added gradually. Mixing continued for an additional 4 min to ensure a uniform consistency. The fresh mortar was cast into $40 \times 40 \times 160$ mm prisms for both compressive strength testing and durability studies. Compaction was achieved using a vibrating table for 2 min. Post-casting, specimens were labeled by mix designation (LCCA50–H_2O, LCCA50–NaOH, and LCCA50–Na_2SO_4). To prevent moisture loss, molds were covered with impermeable polyethylene sheets and stored at 22 ± 2 °C with a relative humidity exceeding 90% for 24 ± 0.5 h. Following demolding, the specimens were subjected to a controlled ambient air-curing regime for 28 days. This curing method was specifically selected to facilitate atmospheric carbonation, which is essential for the strength development of lime-based binders and the stabilization of the resulting matrix. Throughout this period, the laboratory environment was maintained at a temperature of 22 ± 2 °C and a mean relative humidity of 90 ± 5%. Specimens were arranged with sufficient clearance to ensure uniform exposure to atmospheric CO_2, allowing for the synergistic progression of pozzolanic reactions and carbonation.

2.2.6 Compressive strength determination

The compressive strength of the lime–CCA mortars was determined in accordance with KS EAS 148-1:2000 [45]. Upon reaching the 28-day curing age, compressive strength tests were conducted using a calibrated compressive strength machine (Model No. SSC-546). The prisms were subjected to direct compressive loading in accordance with the instrument's operational manual, with the load applied uniformly to the lateral faces at a constant rate of 2400 ± 200 N/s until failure. To ensure statistical accuracy and

Table 1 Characteristics of the binder mixtures

Mix ID	% Composition by Weight	Mixture	Formulations
	Lime (%)	CCA (%)	Binder–Liquid System
LCCA50	50	50	LCCA50–H_2O
			LCCA50–0.5 M NaOH
			LCCA50–0.5 M Na_2SO_4
L100	100	0	L100–H_2O

reproducibility of the results, the final compressive strength for each mix was recorded as the average of triplicate measurements. The relative impact of chemical activation on the compressive strength of the mortars was quantified at 28 days using the percentage change (ΔC), calculated according to Eq. (1):

$$\Delta C = \frac{Cact - CH_2O}{CH_2O} \times 100 \quad (1)$$

ΔC = percentage change in compressive strength (%), C_{act} = compressive strength of chemically activated mortars (LCCA50–0.5 M NaOH or LCCA50–0.5 M Na_2SO_4) at 28 days, and C_{H_2O} = compressive strength of non-activated mortar (LCCA50–H_2O) at 28 days.

2.2.7 Determination of Porosity

The effective porosity of the mortar specimens was determined at the 28-day curing age using the water displacement method. The porosity was calculated using Eq. (2):

$$P = \frac{Wa - Wb}{Wa - Wc} \times 100 \quad (2)$$

where *P* is the effective porosity (%), *Wa* is the weight of the specimen in the saturated surface-dry condition, *Wb* is the oven-dry mass of the specimen, achieved by drying at 105 ± 5 °C until a constant weight is recorded, and *Wc* is the apparent mass of the saturated specimen when weighed while suspended in water.

2.2.8 Resistance to sulfuric acid attack

The resistance of the mortars to chemical degradation was evaluated in accordance with ASTM C267:1997 [46], with minor modifications to specimen geometry. Mortar prisms of dimensions 160 × 40 × 40 mm were utilized to assess the impact of varying acid concentrations on the binder matrix. Following the initial 28-day air-curing period, the specimens were divided into two groups and submerged in sulfuric acid solutions at concentrations of 0.5% and 3.0% by volume. This dual-concentration approach was adopted to compare the effects of mild versus aggressive acidic environments on the durability of the lime–CCA system. The solutions were maintained at a controlled temperature of 23 ± 1 °C. To prevent the neutralization of the acid by the alkaline components of the mortar and to maintain a constant corrosive environment, the solutions were renewed weekly to ensure a stable pH throughout the 28-day exposure period. At the conclusion of the immersion period, the specimens were removed, rinsed with tap water, and carefully brushed with a soft nylon brush to remove loose corrosion products. The prisms were then oven-dried for 3 h before determining their final mass and residual compressive strength. The percentage residual weight (Rw) and residual strength (Rs) were calculated using Eqs. (3) and (4), respectively.

$$R_w = \frac{Wa - Ws}{Wa} \times 100 \quad (3)$$

$$R_s = \frac{Ci - Ct}{Ci} \times 100 \quad (4)$$

where W_a is the weight of the specimen before acid exposure (g), W_s is the weight of the specimen after acid exposure (g), C_i is the initial compressive strength at 28 days (MPa), and C_t is the compressive strength after 28 days of acid immersion (MPa). The results reported represent the arithmetic mean of triplicate measurements for each mix designation at both concentration levels.

3 Results and discussion

3.1 Physical and chemical composition analysis

The composition of CCA and HL used in this study is given in Table 2.

The chemical composition of CCA demonstrates strong pozzolanic potential. This is mainly due to its high SiO_2 content, which is the dominant reactive oxide. CCA is an artificial pozzolanic material that reacts with calcium hydroxide in the presence of moisture at ordinary temperatures to form cementitious compounds [47, 48]. The chemical analysis confirms that the ash contains high levels of reactive silica. It also satisfies the ASTM C618: 2015 [49] requirement for pozzolanic materials, which specifies that the combined SiO_2 + Al_2O_3 + Fe_2O_3 content must exceed 70%. Studies by Okeke et al. [17]. and Umar and Musa [14] also reported oxide sums above 70%, supporting the classification of CCA as a Class N pozzolan. This agrees with the findings of the present study.

The combined SiO_2 + Al_2O_3 + Fe_2O_3 content obtained in this study is higher than the pozzolanic oxide content of CCA reported by Fadele and Otieno [30] but lower than what was reported by Abioye et al. [50]. Differences in oxide composition reported in the literature are likely due to variations in combustion temperature, burning duration, and the source of the corn cob. In contrast, HL is dominated by CaO. This confirms its role as the main source of $Ca(OH)_2$ during hydration. The high CaO content in HL provides the alkaline environment needed to initiate and sustain the pozzolanic reaction with CCA [7]. Silica is the main pozzolanic constituent in CCA and is expected to react with $Ca(OH)_2$ to form C–S–H gel, the reaction product widely reported to drive strength development and matrix densification in lime-pozzolan systems. The Al_2O_3 content (7.13%) and Fe_2O_3 content (3.45%) also contribute reactive aluminosilicate phases. Reactive alumina is expected to promote the formation of C–A–H, phases reported to complement C–S–H and contribute to pore refinement in comparable systems [51], although their presence was not directly confirmed in the hardened mortars of this study.

Table 2 Chemical composition and physical properties of CCA and HL

Composition (%)	CCA	HL
SiO_2	61.61 ± 0.1	-
Al_2O_3	7.13 ± 0.02	0.21 ± 0.01
Fe_2O_3	3.45 ± 0.05	-
CaO	9.39 ± 0.05	85.44 ± 0.02
MgO	2.34 ± 0.04	1.34 ± 0.03
P_2O_5	2.84 ± 0.03	-
Na_2O	0.37 ± 0.02	-
K_2O	15.72 ± 0.02	-
LOI	6.58 ± 0.2	25.13 ± 0.03
Mean size (um)	23.21	-
Specific gravity	2.36	2.79

The high K_2O content is typical of biomass ashes. Agricultural plants absorb potassium from the soil during growth. During combustion, organic matter is removed while inorganic potassium compounds remain concentrated in the ash [29]. The K_2O content measured in this study is consistent with the range of 7.83% – 45.7% reported in earlier studies [28, 30]. High alkali content may increase cracking at high replacement levels. This may result from increased alkali activity and enhanced dissolution of siliceous phases during hydration [48]. The CaO content of CCA (9.39%) also suggests the presence of calcium-bearing minerals. These may provide additional calcium ions during pozzolanic reactions.

The chemical composition of CCA has important implications for the application of lime–CCA binders. The relatively high K_2O content indicates significant alkali levels. In lime–pozzolana systems, these alkalis increase the alkalinity of the pore solution. This can accelerate the reaction between hydrated lime and reactive silica. Unlike Portland cement systems, lime– pozzolana binders rely mainly on pozzolanic reactions and carbonation. The reactive silica combines with $Ca(OH)_2$ released from hydrated lime to form secondary binding phases. These phases improve strength and densify the matrix. However, excessive alkali content may affect dimensional stability and long-term durability, especially in the presence of reactive aggregates [48, 52].

The MgO content of 2.34% is low and within acceptable limits. High MgO contents are undesirable because they can cause delayed expansion and unsoundness. The minor oxides Na_2O (0.37%) and P_2O_5 (2.84%) confirm that the ash is predominantly an aluminosilicate–potassium system. The loss on ignition of CCA is 6.58%. This is within the ASTM C618 limit of 10% for pozzolanic materials. The LOI mainly reflects the release of chemically bound water and CO_2 from residual carbonate phases. In this study, the LOI is associated with residual carbonate minerals such as kalicinite, $KHCO_3$, and calcite. This agrees with the XRD findings. Minor unburnt organic matter may also contribute to the LOI. In contrast, HL recorded a high LOI of 25.13%. This is attributed to the removal of chemically bound water and decomposition of carbonate phases during heating [53].

3.2 X-Ray diffractometer (XRD) analysis

Figure 2 presents the X-ray diffraction patterns of MCA.

The XRD pattern of the CCA confirms the strong pozzolanic potential observed in the chemical composition analysis. The diffractogram is dominated by a broad diffuse hump within the low-angle region ($2\theta \approx 15\ ^\circ$–$30\ ^\circ$), indicating a predominantly amorphous structure. This amorphous phase is mainly associated with disordered silica-rich material formed during controlled combustion of the biomass [17]. The absence of sharp and intense crystalline peaks indicates limited long-range atomic ordering. This is desirable because amorphous silica is more reactive than crystalline silica [51, 54].

The dominance of the amorphous hump is consistent with the high SiO_2 content obtained from the elemental analysis. This confirms that a significant portion of the silica exists in a reactive amorphous form rather than as stable crystalline quartz. Minor crystalline peaks corresponding mainly to sylvine (KCl), kalicinite ($KHCO_3$), and calcite ($CaCO_3$) are superimposed on the amorphous background. These phases originate from inorganic minerals naturally absorbed by the corn plant during growth and from secondary reactions occurring after combustion during cooling and storage [30, 31]. The presence of potassium-bearing phases such as KCl and $KHCO_3$ agrees with the high K_2O

content identified in the elemental analysis. Agricultural biomass typically accumulates alkali metals, particularly potassium, from the soil, which remain concentrated in the ash after combustion [29]. Calcite formation is associated with carbonation of calcium-containing compounds after combustion [6].

Although these crystalline phases are relatively inert in pozzolanic reactions, their low peak intensity compared with the amorphous hump indicates that they do not significantly reduce the reactivity of the ash. Excessive crystallinity generally lowers pozzolanic activity because crystalline silica and alumina dissolve more slowly in alkaline environments [55]. In the present study, the limited crystallinity confirms that most of the silica remains in a reactive amorphous state. This supports the high pozzolanic reactivity indicated by the oxide composition.

The potassium-bearing phases may also influence the reaction behavior of the lime-CCA system, as discussed in Sect. 3.3. The presence of Sylvine and calcite aligns with the K_2O and CaO contents identified in the elemental analysis. In biomass ashes, calcium commonly exists as $CaCO_3$ at relatively low combustion temperatures. At higher temperatures, $CaCO_3$ progressively decomposes into CaO, which can subsequently react with SiO_2 and other oxides [52]. The detected calcite therefore indicates the presence of calcium-bearing minerals that may contribute supplementary calcium ions during pozzolanic reactions. The mineralogical composition strongly supports the findings of the elemental analysis and confirms the suitability of CCA as a pozzolanic material for lime-based binder systems.

3.3 Decrease in electrical conductivity

The variation in electrical conductivity drop with respect to time for CCA is presented in Fig. 3.

The electrical conductivity (EC) loss curve of CCA shows a clear biphasic behavior over the 240 min test period. A rapid conductivity loss of about 15.1% occurs within the

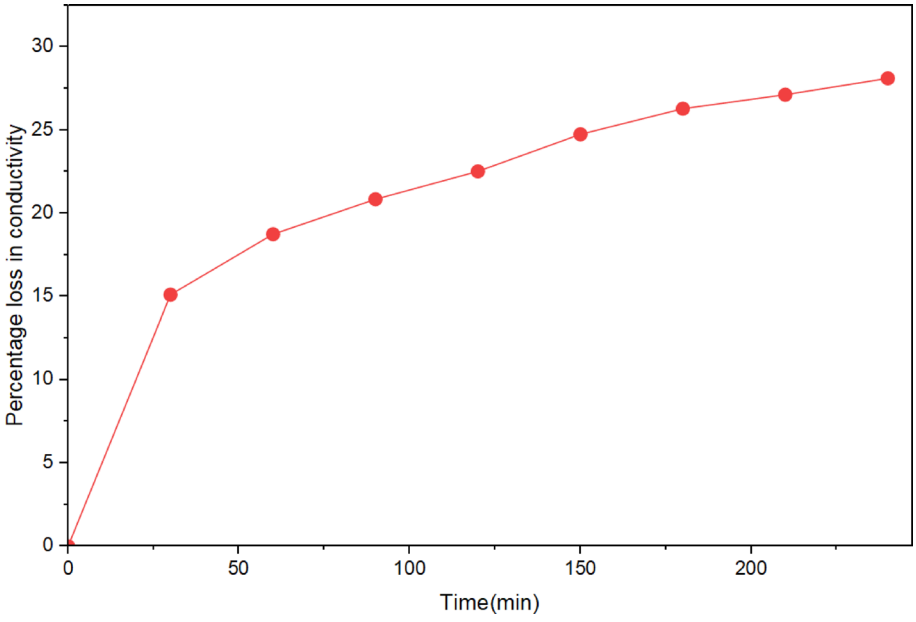

Fig. 3 Electrical conductivity loss of the saturated calcium hydroxide solution containing CCA as a function of reaction time, showing the pozzolanic reactivity of the ash

first 30 min. After this stage, the rate of conductivity loss decreases gradually, reaching a total EC loss of approximately 28.1% at 240 min. The progressive reduction in conductivity indicates continuous consumption of dissolved Ca^{2+} and OH^- ions from the saturated $Ca(OH)_2$ solution through ongoing pozzolanic reactions [56]. The sharp initial decrease in conductivity reflects rapid early-stage reaction kinetics [55].

The high SiO_2 content, together with the broad amorphous hump, confirms the predominance of reactive amorphous silica responsible for this behavior. The relatively fine particle size of the CCA also increases the available reactive surface area, thereby promoting rapid dissolution and early pozzolanic activity [51]. Beyond 30 min, the rate of conductivity loss slows considerably and gradually shifts to a diffusion-controlled regime. The gradual reduction in reaction rate is consistent with the progressive formation of gel layers, likely comprising C–S–H and C–A–S–H, around the CCA particles. As reported for similar pozzolanic systems, these gels can act as diffusion barriers that slow further reaction. These gel products act as physical diffusion barriers. As the gel layer thickens, Ca^{2+} and OH^- ions must diffuse inward through the reaction products to reach unreacted particle surfaces. At the same time, dissolved silicate species must diffuse outward to react with calcium ions in solution. Both diffusion processes become increasingly restricted with time, resulting in slower reaction kinetics [54, 56].

Despite the slower reaction rate at later stages, the conductivity curve continues to decline without reaching a plateau within 240 min. This indicates that residual reactive amorphous silica in the CCA continues to consume Ca^{2+} and OH^- ions beyond the test duration. The high K_2O content identified in the elemental analysis may also contribute to this behavior. Soluble potassium phases such as KCl dissolve rapidly when CCA is introduced into the $Ca(OH)_2$ solution. The released K^+ ions increase the alkalinity of the pore solution, which enhances silica dissolution and promotes faster nucleation of C–S–H during the early stages of reaction [57]. Similar relationships between amorphous silica content, ionic consumption, and conductivity reduction have been widely reported for agricultural ashes and natural pozzolans [42, 54, 58].

The total EC loss of 28.1% at 240 min indicates moderate to good pozzolanic reactivity for CCA. This value is slightly below the 30% threshold commonly reported for highly reactive pozzolans in saturated lime conductivity tests [55]. Compared to other agricultural ashes, the reactivity of CCA remains significant. For example, rice husk ash often exhibits conductivity losses exceeding 40% because of its higher silica purity and larger surface area [58]. The 28.1% conductivity loss observed for CCA suggests that the system approaches, but does not fully reach, the unsaturation limit within 240 min. This moderate reactivity is consistent with the XRD results, which showed the presence of minor crystalline phases such as sylvine, kalicinite, and calcite that partially dilute the reactive amorphous silica fraction. The LOI value of 6.58% further supports this interpretation, as it indicates the presence of residual carbonate and carbonaceous phases that reduce the effective amount of reactive silica per unit mass of CCA.

3.4 Fourier transformer infrared spectrometer (FTIR) analysis

The FTIR spectrum of CCA is presented in Fig. 4.

The FTIR spectrum of CCA displays several characteristic absorption bands that reflect its chemical composition and pozzolanic reactivity. A prominent broadband is observed in the 3400–3563 cm^{-1} region. This is attributed to O–H stretching vibrations

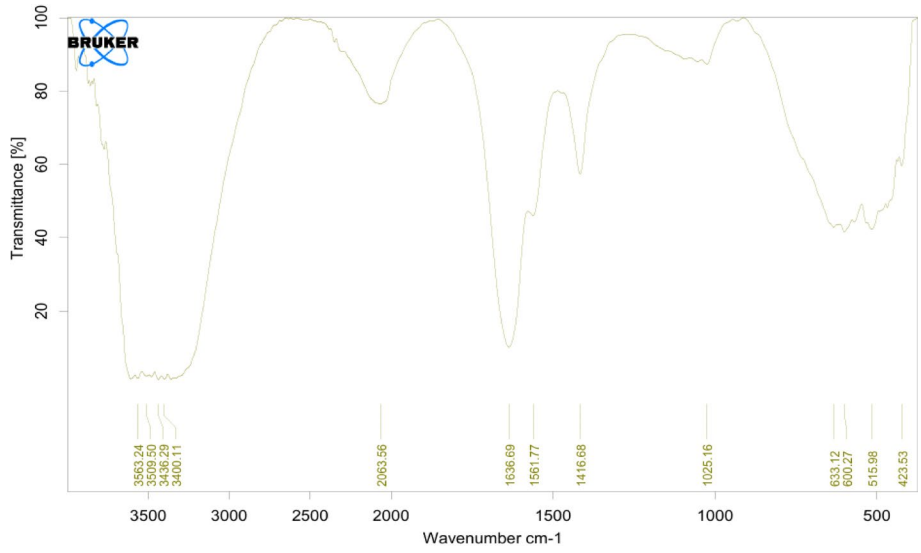

Fig. 4 FTIR spectrum of CCA

associated with structural silanol (Si–OH) groups and physically adsorbed water [59]. This feature indicates the presence of surface hydroxyls and bound moisture, both of which are important for dissolution processes during pozzolanic reactions. The presence of distinct sub-peaks at 3563.24, 3509.50, and 3436.29 cm^{-1} suggests multiple hydrogen-bonding environments [47]. The shift toward lower wavenumbers reflects stronger intermolecular interactions between water molecules and the ash surface [60].

A weak band around 2063 cm^{-1} is associated with overtone or combination vibrations, which may be linked to residual organic compounds or minor carbonate species. Although of low intensity, this band suggests incomplete combustion of the biomass or the presence of trace carbonaceous material [60]. This is consistent with the slightly high LOI of the CCA used in this study. The sharp peak at 1636.69 cm^{-1} corresponds to the H–O–H bending vibration of physically adsorbed water, further confirming moisture retention within the ash [61]. The band at 1561.77 cm^{-1} may be attributed to asymmetric stretching of CO_3^{2-} groups, indicating partial carbonation due to atmospheric CO_2 interaction after calcination. This interpretation is supported by the more pronounced band around 1416 cm^{-1}, which is widely assigned to CO_3^{2-} stretching vibrations [62]. Such carbonate-related bands are commonly reported in biomass ashes and are typically associated with the reaction of calcium-bearing phases with CO_2.

In the fingerprint region, the dominant band at 1025.16 cm^{-1} is assigned to the asymmetric stretching vibrations of siloxane (Si–O–Si) bonds [50]. This is the principal diagnostic peak for CCA, indicating the presence of a silica-rich framework. The presence of this peak suggests a disordered or amorphous silica structure, which is known to enhance reactivity with calcium hydroxide. Lower wavenumber bands at 633.12 cm^{-1}, 600.27 cm^{-1}, and 515.98 cm^{-1} correspond to Si–O bending and O–Si–O deformation vibrations [47]. Additionally, the band near 423.53 cm^{-1} is attributed to Si–O rocking vibrations, further confirming the presence of silicate phases within the ash [59].

3.5 Compressive strength at 28th day of curing

The compressive strength (MPa) of various binder formulations, highlighting the significant increase in mechanical performance achieved by substituting water with chemical activators in the LCCA50 mixtures compared to the L100 control, is presented in Fig. 5.

The compressive strength results exhibit a clear progression: L100–H_2O < LCCA50–H_2O < LCCA50–0.5 M Na_2SO_4 < LCCA50–0.5 M NaOH, highlighting differences in the dominant binding mechanisms within each system. The pure lime mortar (L100–H_2O) shows the lowest strength, primarily due to its reliance on carbonation, where atmospheric CO_2 reacts with $Ca(OH)_2$ to form $CaCO_3$ [7]. This mechanism is inherently slow and surface-controlled and does not generate hydraulic binding phases such as C–S–H [34]. Consequently, strength development remains limited, consistent with the very low compressive strength typically reported for non-hydraulic lime mortars under ambient curing conditions [8, 11].

The inclusion of CCA in LCCA50–H_2O mortar resulted in a 51.91% increase in compressive strength. This improvement is consistent with the pozzolanic reactivity of CCA, where reactive silica is expected to react with $Ca(OH)_2$ to produce additional cementitious phases. These phases refine the matrix and enhance its density, as reported for similar lime–pozzolan systems [9, 47]. This trend is widely documented in lime–pozzolan systems, where strength increases due to the formation of secondary reaction products [51]. However, when water is the sole mixing medium, the relatively low alkalinity limits silica dissolution, thereby constraining the extent of the pozzolanic reaction and the overall strength gain. Previous studies confirm that strength development in such systems is gradual and dependent on the availability of reactive phases [9, 12].

Chemical activation further enhances strength development. The Na_2SO_4-activated system (LCCA50–0.5 M Na_2SO_4) demonstrates a significant increase in strength, rising from 2.91 to 5.92 MPa at 28 days compared to the water-mixed system (LCCA50–H_2O), indicating accelerated reaction kinetics. The strength improvement observed with Na_2SO_4 activation is consistent with the proposed formation of ettringite through the reaction of sulfate ions with aluminum-bearing phases in the ash. As reported for similar

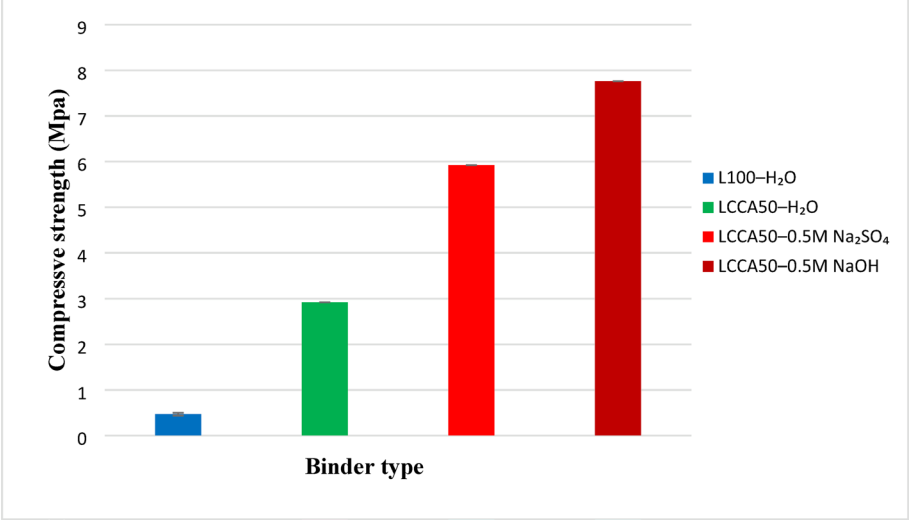

Fig. 5 Compressive strength of the different lime–CCA mortar formulations after 28 days of curing, illustrating the effect of NaOH and Na_2SO_4 chemical activation

activated systems, this reaction can increase solid volume, fill pore spaces, and densify the microstructure, thereby enhancing early-age strength [32, 34–36, 38]. In the present study, this mechanism is proposed based on the observed strength development and existing literature and was not directly verified through phase analysis of the hardened mortar.

The highest compressive strength (7.77 MPa) was achieved with NaOH activation. Sodium hydroxide significantly increases the OH^- concentration in the pore solution, thereby elevating the system pH [39]. The highly alkaline environment is expected to promote the dissolution of the amorphous silica in CCA, thereby accelerating the pozzolanic reaction [63]. Based on findings from comparable alkali-activated systems, this enhanced reactivity is likely to increase the formation of C–S–H, the primary cementitious phase responsible for strength development. The high OH^- concentration attacks Si–O–Si bonds within the glassy CCA phase, liberating silicate ions that react with Ca^{2+} from lime to precipitate substantial amounts of C–S–H [23, 64]. The superior performance of NaOH relative to Na_2SO_4 is consistent with existing literature, where higher alkalinity is associated with increased pozzolanic reactivity and enhanced strength development [38, 61].

The superior compressive strength of the chemically activated lime–CCA mortars is consistent with the physicochemical characteristics of the corn cob ash. XRF analysis showed that the ash was rich in reactive silica but contained relatively low alumina, indicating that silica was the primary reactive component. The XRD pattern further suggested that this reserve is predominantly amorphous (broad hump at $2\theta \approx 15°–30°$, with only minor crystalline sylvine, kalicinite, and calcite peaks). The FTIR spectrum confirms a disordered silicate framework through the dominant Si–O–Si stretching band at 1025.16 cm^{-1} and associated Si–O bending/rocking vibrations. Under alkaline conditions, the amorphous phases are expected to dissolve and react with calcium hydroxide released from hydrated lime to form cementitious hydration products. NaOH, which directly targets Si–O–Si bond cleavage, produced the highest compressive strength (7.77 MPa), likely because its highly alkaline environment more effectively promoted the dissolution of the abundant amorphous silica [65]. In comparison, the lower alumina content (7.13% by XRF) may have limited ettringite formation in the Na_2SO_4-activated system, resulting in a lower, though still improved, compressive strength (5.92 MPa).

Statistical analysis using one-way ANOVA revealed highly significant differences among the four mixes ($p < 0.0001$), while Welch's t-test confirmed that each successive increase in strength from L100–H_2O to LCCA50–H_2O, LCCA50–0.5 M Na_2SO_4, and LCCA50–0.5 M NaOH was statistically significant ($p < 0.0001$). These results confirm that the observed improvements in compressive strength due to CCA incorporation and chemical activation are robust and not the result of experimental variability.

To assess their practical applicability, the compressive strengths were compared with the classification for rendering and plastering mortars specified in BS EN 998-1:2016 [66], which defines four strength classes: CS I (0.4–2.5 MPa), CS II (1.5–5.0 MPa), CS III (3.5–7.5 MPa), and CS IV (> 6 MPa). Based on this classification, the non-activated LCCA50–H_2O mortar (2.91 MPa) falls within the CS II category, making it suitable for general-purpose internal plastering and low-demand rendering applications. The Na_2SO_4-activated mortar (5.92 MPa) approaches the upper limit of CS III, indicating its suitability for more demanding rendering and plastering applications. The

NaOH-activated mortar achieved the highest compressive strength (7.77 MPa), exceeding the minimum requirement for the CS IV classification. These results demonstrate that chemical activation, particularly with NaOH, substantially enhances the engineering performance of lime–CCA mortars, enabling them to satisfy the highest strength class specified in BS EN998-1:2016 for rendering and plastering mortars. This highlights their potential for non-structural applications such as renders, plasters, masonry mortars, and architectural finishes where moderate strength and durability are required.

Despite these improvements, the highest compressive strength obtained (7.77 MPa) remains considerably lower than the 20–40 MPa typically reported for conventional ordinary Portland cement (OPC) concretes used in structural applications. This reflects the inherently slower pozzolanic reaction kinetics and lower binder reactivity of lime–CCA systems compared with Portland cement-based binders. Consequently, the chemically activated lime–CCA mortars developed in this study should not be regarded as substitutes for OPC in structural or heavily loaded applications. Rather, their practical significance lies in providing a more sustainable, low-carbon binder for non-structural construction, including internal and external plastering, non-load-bearing masonry, masonry mortars, paving blocks, curb stones, and the repair and conservation of historic structures, where compatibility with existing substrates, vapor permeability, durability, and reduced embodied carbon are often more important than achieving high compressive strength [6–10].

3.6 Porosity

Figure 6 illustrates the porosity percentages of different binder types, comparing the effects of various mixing liquid mediums on the structural density of L100 and LCCA50 mixtures.

The porosity results exhibit a clear decreasing sequence: L100–H_2O > LCCA50–H_2O > LCCA50–0.5 M Na_2SO_4 > LCCA50–0.5 M NaOH. The pure lime mortar (L100–H_2O) records the highest porosity. This can be attributed to its dependence on carbonation as the principal hardening mechanism. Carbonation involves the diffusion

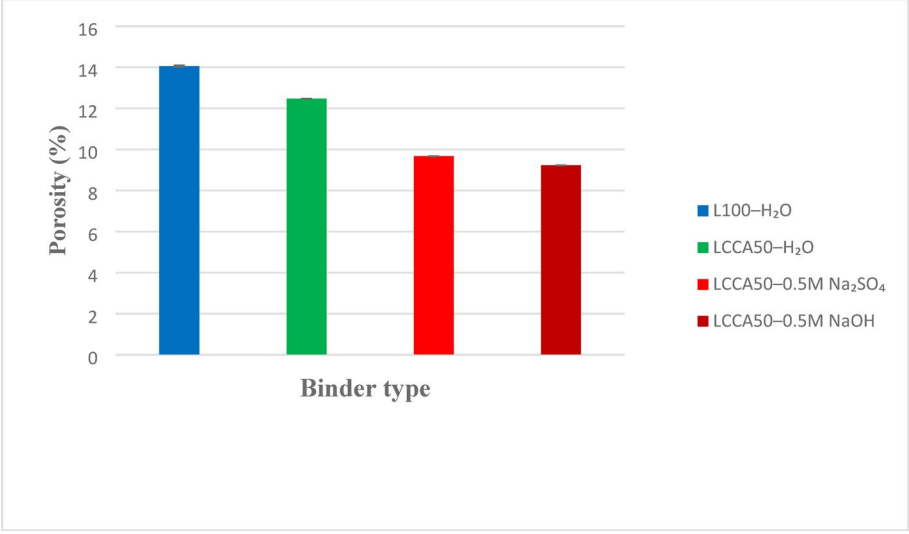

Fig. 6 Effective porosity of the mortar formulations after 28 days of curing, showing the influence of chemical activation on matrix densification

of CO_2 into the pore network and its reaction with $Ca(OH)_2$ to form $CaCO_3$ [6]. This process is inherently slow, surface-controlled, and often incomplete under ambient curing conditions and may lead to a relatively poorly consolidated internal matrix. In the absence of hydraulic reaction products, the pore structure is not effectively refined, instead, evaporation of excess mixing water leaves interconnected capillary voids, resulting in a coarse and open pore network [7, 67].

The incorporation of CCA in LCCA50–H_2O led to a reduction in porosity, primarily due to pozzolanic reactions between reactive silica in CCA and $Ca(OH)_2$ supplied by lime [51]. The reduction in porosity is consistent with the formation of secondary cementitious phases, such as C–S–H, which have been widely reported to densify the matrix and refine the pore structure in comparable lime–pozzolan systems [13, 16]. Furthermore, CCA particles may provide additional nucleation sites for the precipitation of reaction products, enhancing the development of C–S–H and further refining the pore structure [33]. However, as discussed earlier, in water-only systems, the relatively low alkalinity limits the dissolution of silica and consequently restricts the extent of the pozzolanic reaction. As a result, although a reduction in porosity is observed, the improvement remains moderate.

Chemically activated systems (LCCA50–0.5 M Na_2SO_4 and LCCA50–0.5 M NaOH) exhibited a further decrease in porosity, reflecting enhanced reaction kinetics and product formation. As discussed earlier, the introduction of chemical activators increases the dissolution of reactive phases in pozzolanic materials, thereby accelerating the formation of binding products that contribute to pore refinement [34]. Sulfate activation is also expected to promote the formation of additional hydration products, such as ettringite, which have been reported to enhance matrix densification and fill pores at early ages in comparable systems [33]. However, its overall effect is typically less pronounced due to the comparatively lower increase in alkalinity [32, 65]. The early-age formation of ettringite can significantly fill pore spaces, leading to reduced porosity and improved early strength [33]. In contrast, NaOH creates a highly alkaline environment that is expected to enhance the dissolution of amorphous silica and promote the formation of additional cementitious phases. This is likely to produce a denser microstructure with lower pore connectivity, consistent with the lowest porosity measured among the investigated systems [39].

3.7 Acid attack resistance

Figures 7 and 8 depict the percentage loss in strength and percentage loss in weight, respectively, of different LCCA50 binder types when exposed to sulfuric acid at two concentration levels (0.5% and 3%).

The results show a consistent trend in both weight loss and compressive strength loss in all mortar categories exposed to acidic environments. Acid exposure generally causes progressive deterioration of cementitious materials. In acidic media, hydrogen ions react with $Ca(OH)_2$ present in the lime–pozzolana binder through a neutralization process. This reaction reduces the alkalinity of the mortar and promotes dissolution of the binding phases formed within the system. Under sulfuric acid exposure, $Ca(OH)_2$ and other calcium-bearing reaction products are expected to react to form gypsum ($CaSO_4 \cdot 2\ H_2O$), in accordance with the well-established acid attack mechanism in lime-based binders. The gypsum formed is moderately soluble and can gradually dissolve and

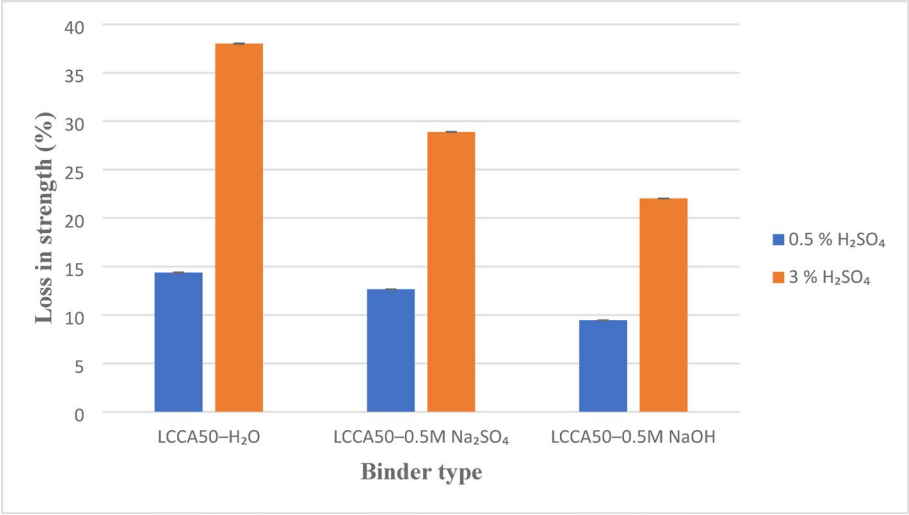

Fig. 7 Percentage compressive strength loss of the mortar formulations after 28 days of exposure to 0.5% and 3% sulfuric acid solutions

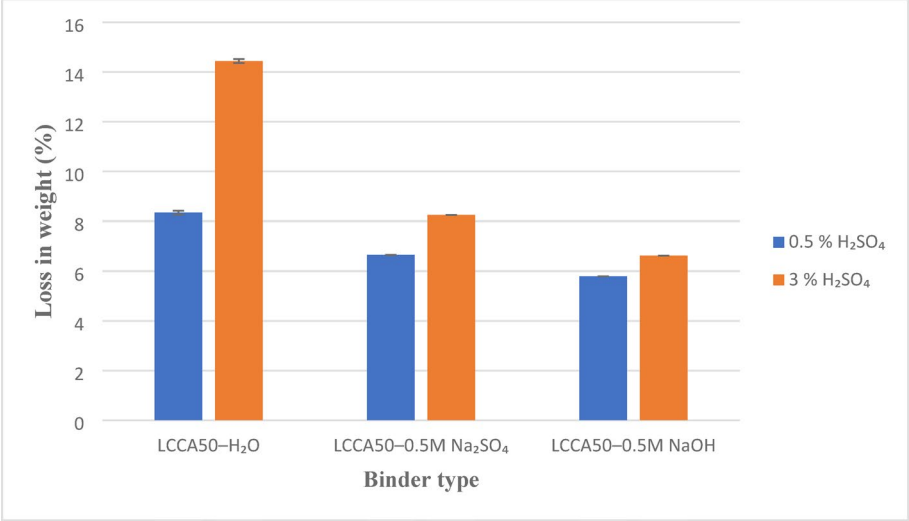

Fig. 8 Percentage weight loss of the mortar formulations after 28 days of exposure to 0.5% and 3% sulfuric acid solutions

leach out of the binder matrix during exposure. This process weakens the lime–pozzolana matrix, increases material degradation, and ultimately leads to reductions in both mass and compressive strength [68, 69].

In this study, the pure lime mortar completely disintegrated after exposure to both sulfuric acid concentrations. This behavior reflects the inherently low acid resistance of non-hydraulic lime systems. The durability of lime-based binders under acidic conditions largely depends on the stability of their hydration and carbonation products. In pure lime mortar, the principal binding phases are $Ca(OH)_2$ and $CaCO_3$, which form through the gradual carbonation of lime [7, 19]. When exposed to H_2SO_4, hydrogen ions aggressively attack these calcium-rich phases, resulting in rapid dissolution and decalcification of the matrix. The acid initially reacts with $Ca(OH)_2$ and subsequently attacks $CaCO_3$, producing soluble calcium bicarbonate and releasing CO_2 gas [70]. Because pure

lime mortar lacks pozzolanic products such as C–S–H that could provide residual structural integrity, dissolution of the carbonate binder leads to complete loss of cohesion and eventual structural collapse. In addition, the absence of dense phases allows rapid acid penetration, which further accelerates degradation and material disintegration [71].

The improved acid resistance of the CCA-containing mortars may be attributed to the formation of C–S–H through pozzolanic reactions. As reported for similar systems, these cementitious phases refine the pore structure and reduce the penetration of aggressive agents [14, 19]. Nevertheless, the water-mixed lime–CCA mortars still recorded higher strength and weight losses than the chemically activated systems. This behavior is consistent with the slower pozzolanic reaction under water-only mixing, which likely leaves a greater amount of unreacted $Ca(OH)_2$ in the matrix. Portlandite is well known to be highly susceptible to sulfuric acid attack, readily reacting to form gypsum ($CaSO_4{\cdot}2\ H_2O$) [33]. Since gypsum is only slightly soluble, it accumulates within the pore network and generates internal stresses. The crystallization pressure associated with gypsum formation induces cracking, spalling, and progressive weakening of the binder structure. Furthermore, the relatively high porosity of the non-activated mortar facilitates deeper acid penetration and accelerates dissolution of calcium-bearing phases. The comparatively lower amount of C–S–H formed in this system provides limited resistance once $Ca(OH)_2$ has been consumed [72, 73].

Chemical activation significantly enhanced the acid resistance of the lime–CCA mortars. The improved acid resistance of the chemically activated mortars reflects the greater C–S–H and ettringite formation discussed in Sect. 3.5 and 3.6. However, although Na_2SO_4 activation improved strength development, it also introduced additional sulfate ions into the matrix. Under acidic conditions, these sulfates can promote secondary ettringite formation and accelerate gypsum crystallization. This often leads to greater expansion and matrix damage compared to the NaOH-activated system. Consequently, Na_2SO_4-activated mortars showed higher strength and weight losses than NaOH-activated mortars [74].

The NaOH-activated mortar exhibited the highest resistance to sulfuric acid attack and recorded the lowest level of deterioration. The strongly alkaline environment created by NaOH enhanced dissolution of reactive silica from CCA, thereby accelerating pozzolanic reactions [75]. This may have resulted in the formation of a denser and less permeable matrix containing larger quantities of stable pozzolanic gels and lower amounts of free $Ca(OH)_2$. The reduction in $Ca(OH)_2$ can minimize the primary phase susceptible to acid attack. Moreover, the higher C–S–H content may have provided improved resistance to dissolution compared with $Ca(OH)_2$ and $CaCO_3$. The lower porosity of the activated system also restricted acid diffusion into the matrix, thereby reducing the depth and rate of deterioration [43, 76].

Across all mortar systems, specimens exposed to 3% H_2SO_4 experienced substantially greater weight and strength losses than those exposed to 0.5% H_2SO_4. This indicates that deterioration severity is strongly dependent on acid concentration. Higher acid concentrations increase the availability of H^+ ions, which accelerate dissolution of calcium-bearing phases such as $Ca(OH)_2$ and $CaCO_3$ and intensify decalcification of C–S–H gels [69]. As decalcification progresses, the binder structure weakens and transforms into a porous silica-rich matrix with little binding capacity. In addition, elevated sulfate concentrations promote faster gypsum formation, resulting in volumetric expansion,

internal stresses, cracking, and severe physical damage. Higher acid concentrations also accelerate diffusion, leaching, and dissolution processes, enabling degradation to penetrate deeper into the mortar matrix and causing greater reductions in both mass and compressive strength. These findings confirm that acid concentration is a major factor controlling deterioration in cementitious and lime–pozzolan systems [73, 76, 77].

The enhanced sulfuric acid resistance of the chemically activated mortars can be attributed to the more effective utilization of the reactive amorphous phases identified by XRF, XRD, and FTIR analyses. Chemical activation, especially with NaOH, is expected to promote the development of a denser and less permeable binder matrix, thereby restricting acid penetration and minimizing deterioration. This is reflected in the lower porosity and reduced mass loss recorded for the activated mortars relative to the non-activated mix. Although the hydration products were not directly identified, the observed durability performance is consistent with the physicochemical characteristics of CCA and the beneficial effects of chemical activation.

Statistical analysis showed that sulfuric acid exposure caused a significant reduction in compressive strength and weight for all mixes compared with their 28-day baseline values ($p < 0.001$). Acid concentration also had a significant effect ($p < 0.001$), with 3% H_2SO_4 producing greater strength loss than 0.5% H_2SO_4. Furthermore, significant differences were observed between the activator systems at each acid concentration ($p < 0.0001$), confirming that the superior acid resistance of the NaOH-activated mortar over the Na_2SO_4-activated and non-activated mortars is statistically robust and reflects genuine differences in activation mechanisms rather than experimental variability.

4 Conclusion

The present study evaluated the pozzolanic potential of CCA and the effect of chemical activation on the performance, porosity, and sulfuric acid resistance of lime–CCA mortars. Based on the experimental findings, the following conclusions can be drawn:

- CCA demonstrated good pozzolanic potential due to its high silica content, predominantly amorphous nature, and observable pozzolanic reactivity, as confirmed by XRF, XRD, FTIR, and electrical conductivity analyses.
- The incorporation of CCA improved the compressive strength of lime mortars relative to pure lime mortar, indicating the positive contribution of pozzolanic reactions within the lime–CCA system.
- Chemical activation significantly enhanced mortar performance, with the compressive strength trend following: L100–H_2O < LCCA50–H_2O < LCCA50–0.5 M Na_2SO_4 < LCCA50–0.5 M NaOH.
- Among the activated systems, NaOH activation produced the highest compressive strength and the lowest porosity, suggesting more effective activation of the lime–CCA binder than Na_2SO_4 activation.
- The decrease in porosity observed in the activated mortars corresponded well with the improvement in compressive strength after 28 days of curing.
- Sulfuric acid exposure caused noticeable deterioration in all mortars, with 3% H_2SO_4 producing greater strength and weight losses than 0.5% H_2SO_4.
- Pure lime mortar showed the poorest acid resistance and completely disintegrated during acid exposure, whereas lime–CCA mortars exhibited comparatively improved resistance to acidic conditions.

- Chemically activated mortars recorded lower strength and weight losses than the non-activated lime–CCA mortar, with the NaOH-activated system demonstrating the best overall resistance to sulfuric acid attack.
- The results indicated that chemically activated lime–CCA binders are more appropriate for non-structural and low-load applications such as plastering mortars, masonry mortars, paving blocks, decorative products, and conservation materials.
- This study contributes to sustainable construction research by demonstrating the potential of agricultural waste-derived CCA as a supplementary pozzolanic material for lime-based binders.
- The findings also highlight the sustainability potential of chemically activated lime–CCA binders. Replacing 50% of hydrated lime with corn cob ash reduces the use of calcined binder while valorizing an abundant agricultural waste, which is expected to lower the embodied carbon of the binder. Although the environmental benefits were not quantified in this study, the results suggest that chemically activated lime–CCA binders are promising low-carbon alternatives for non-structural construction applications. Future research should validate these benefits through comprehensive life cycle and carbon footprint assessments.
- This study was limited to a single corn cob ash replacement level (50%) and activator concentration (0.5 M), both selected based on previous literature rather than optimization experiments. Therefore, although the results provide a reliable comparison of NaOH and Na_2SO_4 activation, they do not identify the optimum mix proportions for the lime–CCA binder system. Future research should investigate a range of replacement levels and activator concentrations to optimize binder performance.
- This study assessed durability only under sulfuric acid exposure, providing an initial evaluation of the long-term performance of chemically activated lime–CCA mortars. Future research should investigate additional durability properties, including water absorption, sulfate and chloride resistance, freeze–thaw performance, carbonation, and long-term field exposure, alongside microstructural and life cycle assessments, to fully establish their suitability for sustainable construction applications.
- Direct microstructural characterization of the hardened mortars was not performed in this study. Future research should incorporate techniques such as SEM, TG/DTA, and EDS to identify hydration products, assess pore structure refinement, and provide a deeper understanding of the mechanisms responsible for the improved mechanical performance and durability of chemically activated lime–CCA binders.
- The present study evaluated the mechanical and durability performance of chemically activated lime–CCA mortars after 28 days of curing. Future research should examine longer curing periods (56, 90, and 180 days) to assess long-term strength development and durability, considering the continued pozzolanic reactions and carbonation that occur in lime–pozzolan systems.

Acknowledgements
This study was made possible through the support provided by several institutions during both the experimental phase and the preparation of this manuscript. The author gratefully acknowledges these institutions for access to scholarly resources, library materials, laboratory facilities, and consumables, particularly the University of Eldoret, Jomo Kenyatta University of Agriculture and Technology, and Eldoret National Polytechnic, Kenya.

Author contributions
Odiwuor V.O. conceptualized and conducted the data collection, methodology, and writing; Stephene S.B. and Zippora O. conducted supervision, reviews, and editing.

Funding
This research received no specific grant from any funding agency in the public, commercial, or not-for-profit sectors.

Data availability
The datasets generated and/or analyzed during the current study are publicly available in the Zenodo repository at https://doi.org/10.5281/zenodo.21997631.

Declarations

Ethics approval and consent to participate
Not applicable.

Consent for publication
Not applicable.

Competing interests
The authors declare no competing interests.

Received: 11 May 2026 / Accepted: 20 August 2026
Published online: 26 August 2026

References

1. Izumi Y, Iizuka A, Ho H-J. Calculation of greenhouse gas emissions for a carbon recycling system using mineral carbon capture and utilization technology in the cement industry. J Clean Prod. 2021;312:127618.
2. Chaudhury R, Sharma U, Thapliyal PC, Singh LP. Low-CO2 emission strategies to achieve net zero target in cement sector. J Clean Prod. 2023;417:137466.
3. AL-Ameeri AS, Rafiq MI, Tsioulou O, Rybdylova O. Impact of climate change on the carbonation in concrete due to carbon dioxide ingress: experimental investigation and modelling. J Build Eng. 2021;44:102594.
4. Akintayo BD, Babatunde OM, Akintayo DC, Olanrewaju OA. Transforming Industrial Waste into Low-Carbon Cement: A Multi-Criteria Assessment of Supplementary Cementitious Materials for Sustainable Concrete Design. Recycling. 2025;10(6):211.
5. Hossain MU, Cai R, Ng ST, Xuan D, Ye H. Sustainable natural pozzolana concrete–a comparative study on its environmental performance against concretes with other industrial by-products. Constr Build Mater. 2021;270:121429.
6. Török Á, Kis A. Carbonation process of commercial lime mortars vs. cement-based mortars: comparative analysis of textural differences, strength, and durability. MATEC Web Conf. 2024;403:02001.
7. Silva BA, Guerreiro E, Duarte APC. Comparative study of lime-based mortars for conservation and restoration interventions. Constr Build Mater. 2025;499:143956.
8. Wang X, et al. Enhancing hydraulic lime mortar with metakaolin: a study on improving restoration materials for historic buildings. Materials (Basel, Switzerland). 2024;17(14):3548.
9. İsafça-Kaya T, Mardani A, Doğangün A, Kaya Y. Improving Lime-Based Restoration Mortars: Effect of Type and Utilization Rate of Binder and Aggregate. Materials. 2025;18(5):961–961.
10. Loureiro S, Patrícia S, Do M, Angélica RS. Assessment of compatibility between historic mortars and lime-METAKAOLIN restoration mortars made from Amazon industrial waste. Appl Clay Sc. 2020;198:105843.
11. Biswas D, et al. A review on agricultural waste ashes as sustainable supplementary cementitious materials for concrete applications. Discover Concrete Cem. 2026;2(1):25.
12. Malathy R, Chung I-M, Kim SH, Prabakaran M, Shanmugam R. Mechanical and microstructural properties of composite mortars with lime, silica fume, and rice husk ash. Processes. 2022;10(7):1424–1424.
13. Onsongo SK, Olukuru J, Munyao OM, Mwabonje O. The role of agricultural ashes (rice husk ash, coffee husk ash, sugarcane bagasse ash, palm oil fuel ash) in cement production for sustainable development in Africa. Discover Sustain. 2025;6(1):62.
14. Umar AA, Musa UA. Durability Performance of Corn Cob Ash–Coconut Shell Ash Concrete Exposed to Simulated Oil Refinery Wastewater. J Civil Eng Front. 2025;6(02):58–69.
15. Mirzaei L, Ghebrab T, Fedler CB. Review and evaluation of agricultural biomass ashes as supplementary cementitious materials for sustainable concrete. Processes. 2025;13(11):3571.
16. Devadharshini M, Vasugi K. A Comprehensive Review and Future Directions on the Utilization of Agricultural Waste Ash in Geopolymer Concrete. Int J Eng Trends Technol (IJETT). 2025;73(9):125–40.
17. Okeke FO, Ahmed A, Imam A, Hassanin H. Calcination optimization of corncob ash for sustainable cementitious applications: a pathway to low-carbon construction. Sustain. 2025;18(1):311.
18. Onyango OV, Kiplagat A, Okoth MO, Munyao OM. Using pozzolanic materials to improve mechanical properties of lime-based mortar. J Chem. 2026. https://doi.org/10.1155/joch/4670233.
19. Onyango OV, Samita FN, Wetungu MW. Performance and durability of chemically activated lime-based cement blended with rice husk ash. J Chem. 2026. https://doi.org/10.1155/joch/4985053.
20. Onyango OV, Wambu EW, Okoth MO, Kipkemboi PK. Pozzolanic reactivity and mortar performance of sugarcane bagasse and sawdust ashes in lime-based binders. Discover Concrete and Cement. 2026. https://doi.org/10.1007/s44416-026-00093-1.
21. Singh A, Panghal H, Bhadauria SS, Chaudhary S. Valorization of de-oiled sesame and sunflower seed residues as sustainable alternatives to limestone and supplementary cementitious materials in cement matrices. J Sustainable Cement-Based Mater. 2025;15(4):1390–410.
22. Singh A, Panghal H, Rath DK, Kumar R, Chaudhary S. Evaluating the potential of oil seed extract ashes from niger, cotton, and flaxseed as sustainable supplementary cementitious materials. Sustain Energy Technol Assess. 2025;76:104285.

23. Khan MI, Alkharisi MK, Dahish HA. Performance of Sustainable Alkali-activated Mortar Incorporating Natural Pozzolan, Waste Glass Powder, and Polypropylene Fibers. Sustainability. 2025;18(1):53.
24. Khan S, Parveez M, Tantray MA. Alkali-activated Geopolymer Masonry with Metakaolin, GGBS, and Quarry Dust. Pollack Periodica. 2025;20(3):24–30.
25. Khan S, Parveez M, Tantray MA. Self-compacting geopolymer concrete: advances, challenges, and future directions. Chem Pap. 2025;80(4):3257–75.
26. FAO. Food and Agriculture Organization of the United Nations. Annual Corn Production. Rome, Italy: FAO; 2023.
27. Santolini E, Bovo M, Barbaresi A, Torreggiani D, Tassinari P. Turning Agricultural Wastes into Biomaterials: Assessing the Sustainability of Scenarios of Circular Valorization of Corn Cob in a Life-Cycle Perspective. Appl Sci. 2021;11(14):6281.
28. Okeke FO, Ahmed A, Imam A, Hassanin H. Harnessing the bio-structure of corncobs: connecting morphology to mechanical attributes for sustainable building materials. Clean Technol Environ Policy. 2026. https://doi.org/10.1007/s10098-025-03379-3.
29. Karim A, Koteng DO, Ambassah N. Effect of Pretreated Corn Cob Ash on the Mechanical and Durability Characteristics of High-Strength Concrete. Int J Civil Eng. 2024;11(3):125–38.
30. Fadele OA, Otieno MB. Properties of corn cob ash and effect on hydration kinetics in PC-blended cementitious systems. Discover Civil Engineering. 2026. https://doi.org/10.1007/s44290-026-00462-6.
31. Pandey A, Kumar B. Utilization of agricultural and industrial waste as replacement of cement in pavement quality concrete: a review. Environ Sci Pollut Res. 2022;29(17):24504–46.
32. Mwiti MJ, Karanja TJ, Muthengia WJ. Thermal resistivity of chemically activated calcined clay-based cements. RILEM Bookseries. 2017. https://doi.org/10.1007/978-94-024-1207-9_53.
33. Mwiti MJ, Karanja TJ, Muthengia WJ. Properties of activated blended cement containing high content of calcined clay. Heliyon. 2018;4(8):e00742.
34. Shi C, Day RL. Pozzolanic reaction in the presence of chemical activators. Cem Concr Res. 2000;30(1):51–8.
35. Abdullah A, Jaafar MS, Taufiq-Yap YH, Alhozaimy A, Noorzaei J. The effect of various chemical activators on pozzolanic reactivity: a review. Sci Res Essays. 2012;7:719.
36. Marangu JM, Thiong'o JK, Wachira JM. Chloride ingress in chemically activated calcined clay-based cement. J Chem. 2018. https://doi.org/10.1155/2018/1595230.
37. Ngui F, Muhammed N, Mutunga FM, Marangu JM, Otieno M, Mutai VK. Strength and durability performance of hybrid alkaline clay brick waste –coconut shell ash cement. Journal of Sustainable Construction Materials and Technologies. 2024. https://doi.org/10.47481/jscmt.1607846.
38. Zuzhong L, et al. Effect of Alkali and Sulfate on the Hydration Characteristic of Cement-Based Materials Containing Coal Gasification Slag. Materials. 2022;15(24):8868.
39. Wardhono A. The effect of sodium hydroxide molarity on strength development of non-cement class C fly ash geopolymer mortar. J Phys Conf Ser. 2018;947:012001.
40. Zafarana SE, Scanferla P, Finocchiaro C, Galusek D. Influence of activator molarity and waste-glass-to-volcanic-ash ratios on the microstructure of potassium-based alkali-activated pastes. J Sol-Gel Sci Technol. 2025. https://doi.org/10.1007/s10971-025-06937-9.
41. Arif R, Iqtidar A, Khattak SU. Utilizing Corn Cob Ash and Bauxite as One-Part Geopolymer: A Sustainable Approach for Construction Materials. Eng Proc. 2023;44:18.
42. Musyimi NF, Karanja J, Wachira M, Mulwa M. Pozzolanicity and Compressive Strength Performance of Kibwezi Bricks Based on Cement. IOSR J of Appl Chem (IOSR-JAC. 2016;9(2):28–32.
43. Játiva A, Andreu A, Etxeberria M. Durable Mortar Mixes Using 50% of Activated Volcanic Ash as a Binder. Mater. 2025;8:1777.
44. Sales LPB, da Nóbrega AF, da Nóbrega ACV, de Malheiro R, de França MS, Suraneni P. $CaCl_2$ as a hardening accelerator for airlime-metakaolin slurries: effects of two different types of metakaolin on kinetics, rheology, and microstructure. Appl Clay Sci. 2026;292:108302.
45. KS EAS 148. 1, Kenya standard test method for determination of cement strength. Nairobi, Kenya: Kenya Bureau of Standards; 2000.
46. ASTM. Standard Test Methods for Chemical Resistance of Mortars, Grouts, Monolithic Surfacing, and Polymer Concretes. Volume C267–97. West Conshohocken, PA, USA: ASTM; 1997.
47. Abdullah AHD, Chalimah S, Primadona I, Hanantyo MHG. Physical and chemical properties of corn, cassava, and potato starch. IOP Conf Series: Earth Environ Sci. 2018;160:012003.
48. Gebreslassie HL, Cherkos FD, Mitikie BB. Experimental investigation on mechanical, durability, and microstructural sugarcane bagasse fiber reinforced concrete with partial replacement of cement by corn waste ash. Discover Civil Engineering. 2025. https://doi.org/10.1007/s44290-025-00283-z.
49. ASTM C618-15. Standard Specification for Coal Fly Ash and Raw or Calcined Natural Pozzolan for Use in Concrete. American Society for Testing and Materials (ASTM): West Conshohocken, PA, USA, 2015.
50. Abioye AA, Olutoge FA, Ofuyatan OM, Oyebisi SO. Effect of corncob ash blended cement on the properties of lateritic interlocking blocks. Progress Industrial Ecol Int J. 2017;11(4):373.
51. Walker R, Pavía S. Physical properties and reactivity of pozzolans, and their influence on the properties of lime–pozzolan pastes. Mater Struct. 2010;44(6):1139–50.
52. Chen H-J, Shih N-H, Wu C-H, Lin S-K. Effects of the loss on ignition of fly ash on the properties of high-volume fly ash concrete. Sustainability. 2019;11(9):2704.
53. Hernández García LC, Colorado Lopera HA. Effect of the loss on ignition on the unconfined compressive strength of residual clays from Bogotá- Colombia stabilized with cement. J Mater Res Technol. 2024;33:7123–35.
54. Velázquez S, Monzó J, Borrachero M, Payá J. Assessment of pozzolanic activity using methods based on the measurement of electrical conductivity of suspensions of Portland cement and pozzolan. Materials (Basel). 2014;7(11):7533–47.
55. Payá J, Velázquez S, Borrachero MV, Monzó J. The chemical activation of pozzolanic reaction of fluid catalytic cracking catalyst residue (FC3R) in lime pastes. Adv Cem Res. 2007;19(1):9–16.
56. Fernandes IV, Barbosa DJC, Nascimento CFG, Santos MD, Cartaxo M, Neto AAM. Assessment of the pozzolanic activity of supplementary cementitious materials through electrical conductivity: a systematic methodological review with a scientometric approach. J Build Pathol Rehabil. 2026. https://doi.org/10.1007/s41024-026-00804-y.

57. Kim H, Yoon J. Automated mineral identification of pozzolanic materials using XRD patterns. J Mater Civ Eng. 2024. https://doi.org/10.1061/JMCEE7.MTENG-17973.
58. Mboya HA, King'ondu CK, Njau KN, Mrema AL. Measurement of Pozzolanic Activity Index of Scoria, Pumice, and Rice Husk Ash as Potential Supplementary Cementitious Materials for Portland Cement. Adv Civil Eng. 2017;2017:1–13.
59. Horgnies M, Bouillon C, Chen JC. Overview about the use of Fourier transform infrared spectroscopy to study cementitious materials. WIT Trans Eng Sci. 2013. https://doi.org/10.2495/mc130221.
60. Higl J, Hinder D, Rathgeber C, Ramming B, Lindén M. Detailed in situ ATR-FTIR spectroscopy study of the early stages of C-S-H formation during hydration of monoclinic C_3S. Cem Concr Res. 2021;142:106367.
61. Fernández-Carrasco L, Torréns-Martín D, Morales LM, Martínez-Ramírez S. Infrared Spectroscopy in the Analysis of Building and Construction Materials. In: InTech eBooks. 2012.
62. Yusuf MO. Bond characterization in cementitious material binders using Fourier-transform infrared spectroscopy. Appl Sci. 2023;13(5):3353.
63. Ibrahim M, Johari MA, Rahman MK, Maslehuddin M, Dafalla MH. Effect of NaOH Molarity on the Strength and Microstructure of Natural Pozzolan-Based AAC. MATEC Web Conferences. 2018;203:06017.
64. Adewumi A, Ismail M, Ariffin MAM, Yusuf MO, Maslehuddin M. Strength and microstructure of alkali-activated natural pozzolan and limestone powder mortar. Magazine Civil Eng. 2019;8(92):36–47.
65. Mota B, Matschei T, Scrivener K. Impact of NaOH and Na_2SO_4 on the kinetics and microstructural development of white cement hydration. Cem Concr Res. 2018;108:172–85.
66. BS EN 998-1. Specification for mortar for masonry: Rendering and plastering mortar. British Standards Institution, *Bsigroup.com*, 2016.
67. Alvarez JI, et al. RILEM TC 277-LHS report: a review on the mechanisms of setting and hardening of lime-based binding systems. Mater Struct. 2021. https://doi.org/10.1617/s11527-021-01648-3.
68. Chindaprasirt P, Paisitsrisawat P, Rattanasak U. Strength and resistance to sulfate and sulfuric acid of ground fluidized bed combustion fly ash–silica fume alkali-activated composite. Adv Powder Technol. 2014;25(3):1087–93.
69. Marangu JM. Effects of sulfuric acid attack on hydrated calcined clay–limestone cement mortars. J Sustainable Cement-Based Mater. 2020;10:1–15.
70. Raghunathan T. Acid Attack on Lime Mortar. Int J Eng Res Technol. 2022;11:7.
71. Khaled, et al. Acid Resistance of Alkali-Activated Natural Pozzolan and Limestone Powder Mortar. Sustainability. 2022;14(21):14451–14451.
72. Ibrahim M, Salami BA, Algaifi HA, Rahman MK, Nasir M, Ewebajo AO. Assessment of acid resistance of natural pozzolan-based alkali-activated concrete: experimental and optimization modelling. Constr Build Mater. 2021;304:124657.
73. Deb PS, Sarker PK, Barbhuiya S. Sorptivity and acid resistance of ambient-cured geopolymer mortars containing nano-silica. Cem Concr Compos. 2016;72:235–45.
74. Ibrahim M. Durability Performance of Alkali-Activated Natural Pozzolan and Limestone Powder Mortar in Sulfate Environments. Sustainability. 2025;17(12):1–23.
75. Adewumi AA, Yusuf MO, Maslehuddin M, Ismail M. Effect of sodium hydroxide concentration on strength and microstructure of alkali-activated natural pozzolan and limestone powder mortar. Constr Build Mater. 2021;271:121530–121530.
76. Bakharev T. Resistance of geopolymer materials to acid attack. Cem Concr Res. 2005;35(4):658–70.
77. Ariffin MAM, Bhutta MAR, Hussin MW, Mohd Tahir M, Aziah N. Sulfuric acid resistance of blended ash geopolymer concrete. Constr Build Mater. 2013;43:80–6.

Publisher's Note